

## SEISMIC ASSESSMENT OF MASONRY ARCH BRIDGES WITH FIBRE BEAM STRATEGY

M. Kyriakou<sup>1</sup>, D.V. Oliveira<sup>2</sup>, H. Rodrigues<sup>3</sup>

<sup>1</sup>University of Minho, Department of Civil Engineering, Guimarães, PORTUGAL.

<sup>2</sup>ISISE, University of Minho, Department of Civil Engineering, Guimarães, PORTUGAL.

<sup>3</sup>RISCO, School of Technology and Management, Polytechnic Institute of Leiria, Leiria, PORTUGAL.

e-mails: [mariaKyriak.89@gmail.com](mailto:mariaKyriak.89@gmail.com), [danvco@civil.uminho.pt](mailto:danvco@civil.uminho.pt), [hugo.f.rodrigues@ipleiria.pt](mailto:hugo.f.rodrigues@ipleiria.pt)

---

### SUMMARY

The present paper reports the seismic assessment of masonry arch bridges with the application of a fibre beam element methodology based on the OpenSees software. Three case studies are addressed: a single 2-D arch for which a sensitivity analysis is performed providing the best mesh discretization and the constitutive relations of the material used, a multi-span masonry bridge in order to validate the proposed modelling approach against experiments and lastly, a railway masonry arch bridge, examined for its in-plane dynamic behaviour. The seismic capacity of the second bridge is investigated through a nonlinear pushover and a time-history analysis as well as an incremental dynamic analysis, aiming at evaluating the simplicity and accuracy of the fibre beam strategy for minimized computational costs.

**Keywords:** *Masonry arch bridges, fibre beams, seismic assessment, pushover analysis, IDA.*

### 1. INTRODUCTION

Masonry arches being described by a nonlinear behaviour and complexity, make their seismic assessment a difficult task, while it is highly depended on the level of knowledge of their structural and material characteristics which is very important for the decision of the appropriate method of analysis. The evaluation of masonry arches under earthquake ground motion has been first analysed by the mechanism method as implied according to Heyman's theories for infinite compressive strength and zero tensile resistance [1]. Due to the fact that seismic assessment of masonry arch bridges generally requires demanding modelling strategies resulting at very high computational costs, in the present work, the modelling approach using fibre section beam elements was investigated and evaluated for its simplicity and reliability to assess their response under seismic actions.

The organization of the paper has the following structure. First, the fundamentals of the fibre beam element approach are described, adopted by the OpenSees software. The sensitivity analysis carried out on a single 2-dimensional arch indicating the right amount of fibres and beam elements used is presented, while the constitutive law of the material is determined through a simple beam with fibre cross-section, under compression and tension. Following, a validation of the proposed methodology is processed through the calibration of the load-carrying capability and the curvature profile of a three-span

experimental bridge [2], providing a good compromise between accuracy and simplicity. Later on, a more complex case study, of the multi-span Durrães viaduct, is simulated in order to evaluate the exact methodology resorting to OpenSees. As a first step, a modal analysis is performed in order to calibrate the first longitudinal frequency by documented data of a dynamic test. Moreover, a nonlinear pushover analysis proportional to mass is performed, as well as a nonlinear time-history analysis under three different artificially generated accelerograms. Finally, an incremental dynamic analysis is performed, for which a comparison is made between the average IDA curve and the pushover capacity curve resulting to prove the reliability of the fibre beam element approach. The method has proved to provide accurate results for the same amount of time but with less computational costs, due to the simplification of a 1D element and the discretization of the cross-section into fibres, thus being acceptable for a nonlinear dynamic analysis [3].

## **2. FUNDAMENTALS OF THE FIBRE BEAM ELEMENT APPROACH**

### **2.1. The fibre beam model**

In the last century, an equivalent frame approach by means of fibre section beam elements, has been introduced for the seismic assessment of masonry structures based on a simplified modelling strategy. The method has been firstly developed for the analysis of reinforced concrete elements under biaxial and bending loads [4]. New studies now, show that the use of nonlinear fibre-beam frame models represent a good approximation of the behaviour of masonry walls using 1D macro-elements to simulate wall panels [5].

The proposed fibre beam-column element is based on the assumption that the plane sections remain plane after their deformation and that deformations and displacements are generally small. Along the element, the numerical integration of several monitored sections can determine the nonlinear response of the element. In addition, the constitutive laws are implemented through the uniaxial stress-strain relations ( $\sigma$ - $\epsilon$ ) that are assigned to the fibres, modelling the nonlinear flexural and axial behaviour of the materials [5]. For the modelling of multi-span bridges, the simulation is presented with 1D-models and fibre beam sections.

### **2.2. Material's constitutive relations through the OpenSees software**

For assessing the behavior of multispan masonry arch bridges against static and dynamic loads, the Open System for Earthquake Engineering Simulation (OpenSees) software is used, primarily developed by the University of California, Berkeley. The fibre section model is investigated through OpenSees and is constructed by displacement-based beam column elements which are elements with distributed plasticity [6]. For reproducing the nonlinear behaviour of masonry, several constitutive laws initially developed for concrete can be considered, since no original uniaxial masonry material exists. For the scope of this project, Concrete04 is chosen due to fact that it has the ability to include the tensile strength and to modify the initial stiffness, which is of great importance for calibrating the models [7]. The material, based on the Popovics constitutive law, is able to construct a uniaxial material object with degraded linear unloading/reloading stiffness (Karsa-Jirsa) and tensile strength with exponential decay.

To investigate the material's constitutive law, concrete04 [7] is tested on a simply supported beam under compression and tension, with displacement-based beam-column elements and fibre-sections in order to extract the stress-strain ( $\sigma$ - $\epsilon$ ) relations. Fig.1

shows that ductility is improved with increase of the elastic modules or the maximum compression strain, whereas for tension is visible that the change of the compression parameters influences the tensile stress-strain curve from the initial model.

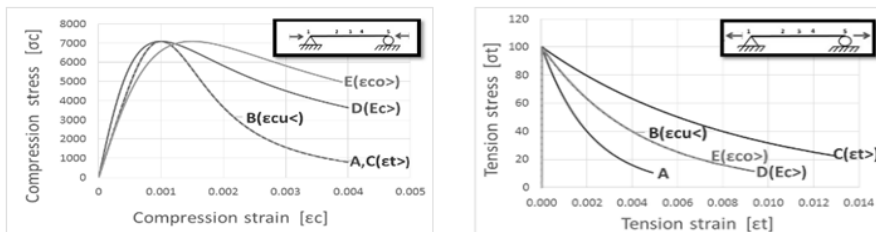


Fig. 1. Stress –strain curves: left - beam under compression; right - beam under tension.

### 3. MODELLING BY THE FIBRE ELEMENT STRATEGY

#### 3.1. Numerical model

The simulation of masonry arch bridges is described by 1D displacement-based beam elements used for the vaults and piers consisted in an in-plane, whereas their cross-sections are defined (in a plane normal to the plane of the structure), by the fibres positioned subdivided only in one direction.

The backfill material has a relatively high weight, providing a structural function of applying some lateral pressure on the arch and contribute to its stability. In the numerical model, the contribution of its stiffness is represented by nonlinear horizontal truss elements, which are also used for the enhancement of the in-plane stiffness provided by the spandrel walls up to the height of the corresponding crowns of the two arches. The connection between arches and pier is modelled by elastic beam elements with an infinite stiffness (rigid links) to assure the existence of a rigid connection, as indicated Fig. 2.

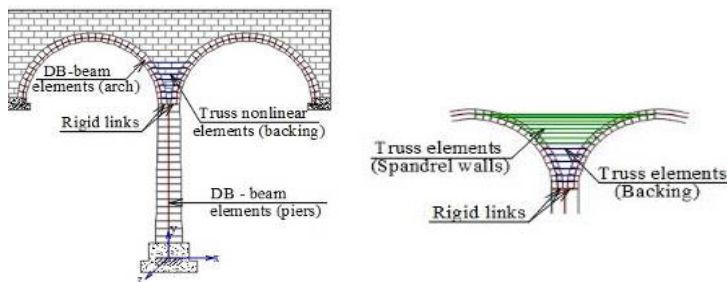
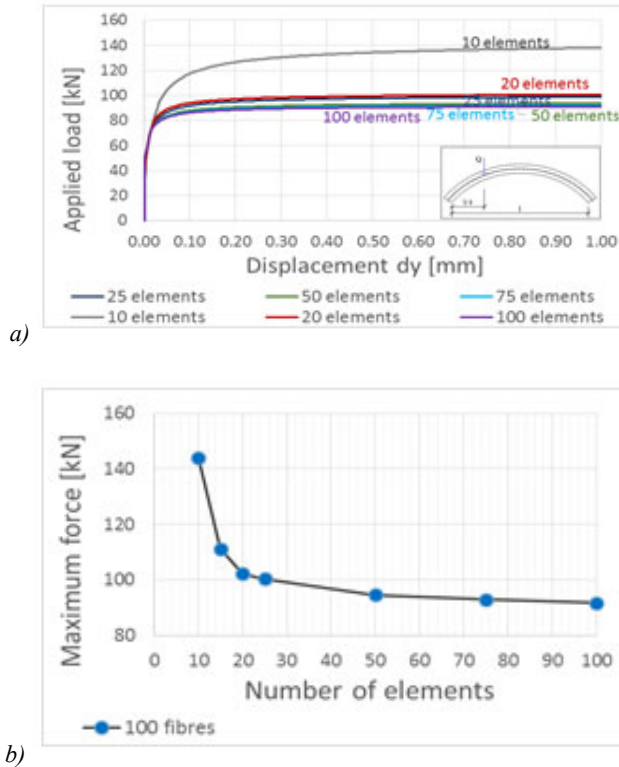


Fig. 2. Modelling masonry arch bridge by means of fibre beam elements.

Lastly, the representation of permanent load from the infill material, the spandrel walls and the arch itself, is implemented for the case of static analysis as nodal loads for the determined self-weight of each element and acting vertically in all nodes respectively.

### 3.2. Sensitivity analysis on a single masonry arch

For the determination of an adequate number of fibres per element's section and elements per arch, a sensitivity analysis is performed for a single arch under displacement control for incremental vertical load at quarter span, applied after the application of the self-weight. Material used is concrete04 but with zero tensile strength.



**Fig. 3.** Sensitivity analysis:

- a) force-displacement curves for models with various number of beam elements;  
 b) relation between number of elements and the corresponding maximum forces.

From the capacity curves it is observed that for a range of beam elements the curve presents an asymptotic behaviour with a decreasing load factor compared to the maximum achieved applied force (Fig. 3). On the contrary, for a variation of number of fibres, the more fibres are used, the highest capacity is achieved. In addition, in the linear range the stiffness seems to be identical, whereas for the nonlinear response, the load-carrying capability is clearly affected by the number of either beam elements or fibres. Finally, a selection of 50 beam elements and 100x1 fibres is made as the most reliable choice, which can lead to an accurate validation of the mesh modelling, proving that the modification of the discretization has a big influence on the structure's maximum capacity as well as the maximum reached displacement.

## 4. VALIDATION OF THE FIBRE BEAM APPROACH

### 4.1. Bolton Institute laboratory test

Based on an experimental work carried out at the Bolton Institute, UK [2], the fibre beam element approach is investigated for multi-span arch bridges with the scope of validating the technique by calibration of known data from tests. The test included three large-scaled bridge models, consisting of three spans each, from which Bridge no. 2 is chosen to be modelled due to the fact that it had the spandrel walls detached from the arch barrels, thus suggesting a clearer simulation. The bridge specimen was constructed with brickwork materials with known both mechanical and geometric properties. In order to assess the load capability, a concrete loading beam was applied approximately at the quarter span of the central arch.

#### 4.1.1. Development of the numerical model

Bridge no. 2 is modelled through fibre beam-column element using 50 fibre beam elements per each arch and 20 beam elements per pier. The number of fibres in the cross-section are discretized into  $100 \times 1$  for both arches and piers based on the mesh validation previously done in order to assure good numerical stability, see section 3.2. Since the entire model simulates the in-plane behaviour of the structure, the cross-section is subdivided only in one direction.

The material assigned to all displacement-based beam elements, for both vaults and piers, follows the same constitutive laws of concrete04, whereas the material characteristics are based on the data given by the experiment. Since there was no information regarding the tensile strength, a value close to 5% of the mean compressive strength of the mortar is chosen, given as  $f_{ct} = 70$  kPa. Furthermore, there was no backing material in the experimental model, therefore it is excluded from the simulation. The fibre beam model is firstly analysed for gravity loads, in which the permanent loads are applied at all nodes considering the self-weight of the infill, spandrel walls and arches. Subsequently, a vertical live load is assigned distributed with a dispersion angle of  $35^\circ$ , by means of displacement control analysis.

### 4.2. Comparison with the experimental model

Following the application of self-weight and increase of the live load, the acting forces and displacements of the control node (at the loaded span) and of the top of the left and right pier are recorded, for which the capacity curves are plotted and compared to the experimental model. From the analysis it was concluded that the elastic modulus of masonry is highly influencing the total behaviour of the bridge. As a result, three models (A, B, C) are adopted in which the first is based on the initial mechanical properties ( $E_{Aca} = E_{Acp} = 16.2$  GPa), whereas models B and C have adjusted elastic modulus for arches and piers with  $E_{Bca} = 10$  GPa,  $E_{Bcp} = 5$  GPa and  $E_{Cca} = E_{Ccp} = 5$  GPa respectively.

The load-displacement relations are represented in Fig.4 for all three numerical models, and compared to the physical one. Numerical analysis provide a failure load slightly higher than the experimental one, whereas model A appears to be much stiffer in the nonlinear pre-peak range since it is the one with the highest elastic modulus, contrary to models B and C which show a better approximation of the nonlinear response. The fibre beam model exhibits a less fragile behaviour leading to a less good estimation of the displacement corresponding to the maximum load. The load-displacement curve of the right pier seems to follow a similar behaviour to the loaded arch node in comparison to

the experimental one, with a better compromise for model C. Contrariwise, the left pier does not provide any significant movement leading to the assumption that probably some damage may had been induced in the model prior to testing. It is worth to mention that previous modelling attempts found a similar behaviour regarding the left pier [8].

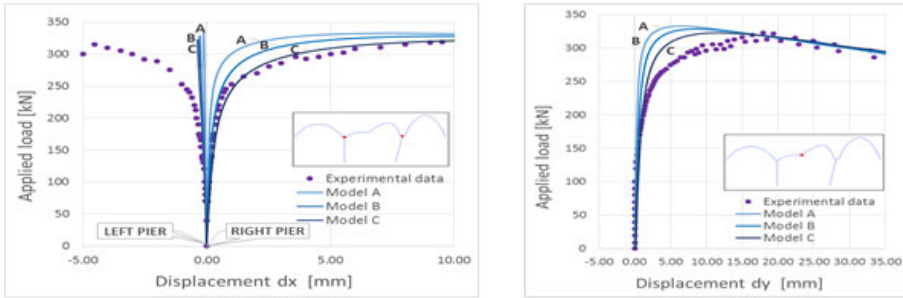


*Fig. 4. Comparison between numerical and experimental models: left - capacity curve of the top nodes of the two piers; right - capacity curve of the node at quarter middle span.*

The failure mode is also investigated for its accuracy and compatibility with the experimental results where a good estimation of the collapse mechanism can demonstrate the reliability of the numerical model. Consequently, the curvature profile is extracted indicating the location of the plastic hinges which are verified by the failure mechanism, and is presented in the Fig. 5.

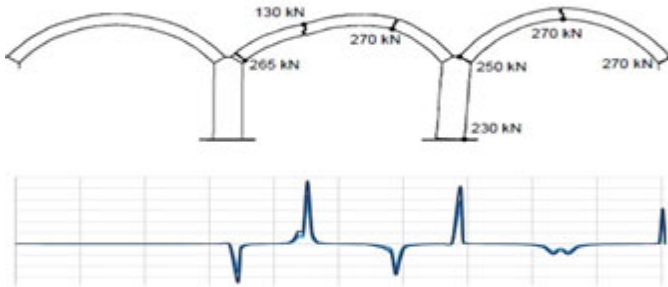


*Fig. 5. Failure mode. Up - experimental failure mode [2]. Down - numerical curvature profile.*

## 5. SEISMIC ASSESSMENT OF A CASE STUDY: DURRÃES VIADUCT

### 5.1. Introduced existing masonry viaduct

The Durrães viaduct, a railway masonry arch bridge in current use, had its construction completed in the 1878. It is located in the north of Portugal and is built mainly of granite

stone masonry. The bridge consists of sixteen semi-circular deep arches ( $r/s = 0.5$ ) of constant thickness 0.6 m and is symmetric along the longitudinal direction with total length of 178 m and constant span length of 9 m. The arches are supported in fifteen piers of differentiated height and non-constant cross-section, two of which more robust. Aiming at investigating the response of a multi-span masonry arch bridge under seismic excitation, the Durrães viaduct is modelled through the fibre beam approach (Fig. 6). The geometry of the model was based on a geometric survey and available documentation.

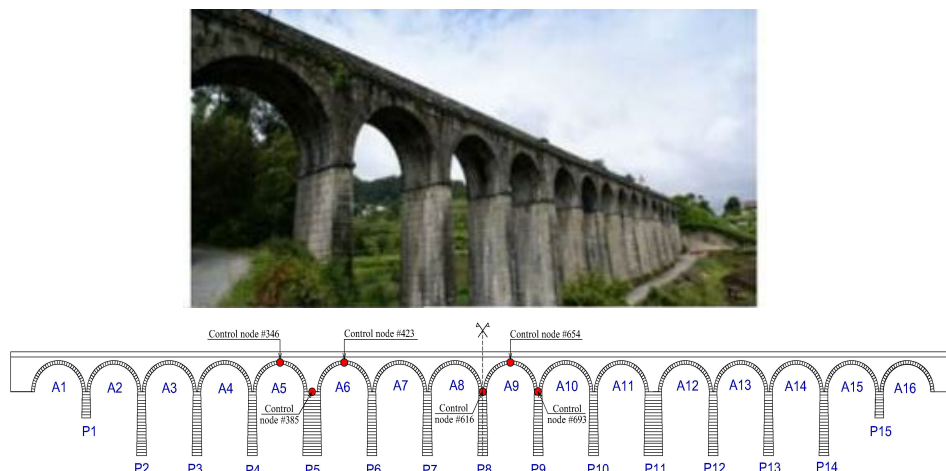


*Fig. 6. Longitudinal view of the Durrães viaduct in the Barcelos area.*

## 5.2. Investigation of the masonry arch bridge under dynamic actions

The 2D computational model is build based on the same methodology and assumptions treated in the previous chapters within the OpenSees software, with the cross-section discretized into 100x1 fibres for both piers and arches for the evaluation of its in-plane behaviour. For the identification of the structure's behaviour under dynamic loading, the simulation of the spandrel walls and the infill soil are of significant importance, thus a new model is adopted, which has nodal forces and modal masses. The masses are positioned in the real barycenter of each voussoir and are connected with rigid links to the nodes of the arch to assure interaction of the masses with the rest of the structure. In order to perform seismic assessment of the case study, the bridge is investigated under dynamic actions by means of modal, pushover and nonlinear dynamic analysis.

### 5.2.1. Modal analysis

As a first step, modal analysis is performed for the calibration of the model with available data obtained from dynamic tests performed in-situ, which are part of an ongoing research project aiming at the experimental identification of the modal parameters of the bridge [9]. With respect to the results from the in-situ dynamic test, a correlation between the dynamic identification test and the numerical model can evaluate

the accuracy of the model for future analysis. Here, only the longitudinal modes and frequencies are compared due to the fact that the numerical model is in the 2D-domain.

A calibration of the 1<sup>st</sup> longitudinal frequency is achieved with adjusting the elastic modulus to  $E_C=13$  GPa, instead of 10 GPa, showing a good correlation between numerical and experimental model with an error of 4.3% (Fig. 7).

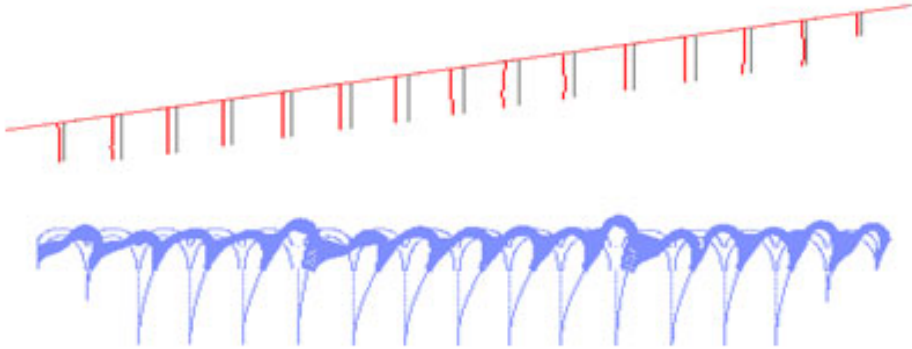


**Fig. 7.** First longitudinal mode shapes: above - obtained by the experimental model:  $f_{1L}=2.50$  Hz [9]; below- obtained by the numerical model:  $f_{1L}=2.396$  Hz.

### 5.2.2. Pushover analysis

Pushover analysis is performed for the most critical control nodes assumed to be the ones presenting the largest displacements observed in the first in plane modal shape. Consequently, the top of the crown of the middle arch, as well as the top nodes of the central piers are more significant to be examined. In-plane incremental horizontal loads proportional to the nodal masses are assigned under displacement control analysis to all nodes, simulating the contribution of arches, piers, infill soil and spandrel walls. The load pattern proportional to the masses is defined by a seismic coefficient  $\alpha$  that relates the sum of the horizontal forces acting on all nodes with the total self-weight of the structure [10].

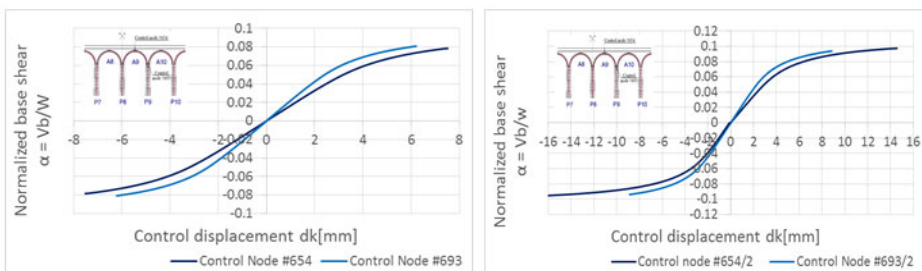


**Fig. 8.** Pushover curves in X-direction for the most critical control nodes: left- case 1; right - case 2.



The capacity curves are extracted for two cases of application point of the nodal masses. In the 2<sup>nd</sup> case the horizontal loads are applied in the nodes of the arches instead of the upper nodes of the rigid links, providing larger displacements.

Adding up to the capacity curves, the curvature profile of the middle pier and the two adjacent symmetrical arches is extracted for the peak load (Fig. 9).

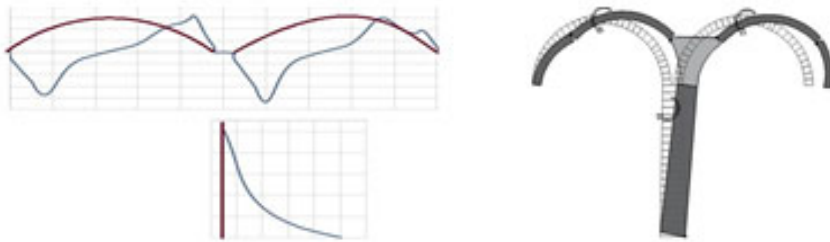


*Fig. 9. Left - Curvature profile for the two central arches and pier under the peak point load; right - schematic illustration of the collapse mechanism.*

The position of the hinges is obtained in the place of the largest deformations (two hinges symmetrically formed in each arch and one in the bottom middle pier). In addition, a schematic illustration of the collapse mechanism is presented from which it is observed that the hinges of the arch are formed exactly above the backing material, thus indicating that the structural member above the top of the pier behaves as a rigid block.

### 5.2.3. Nonlinear incremental dynamic analysis

Durrães viaduct's response under seismic motion is investigated with the performance of incremental dynamic analysis for a series of earthquakes. The analysis consists of performing repeated time-history analysis for adopted accelerograms with an increasing scale factor. In the Barcelos area there are no current available records, therefore three artificial earthquakes were generated based on two types of response spectrums provided by Eurocode 8, one for a far-field scenario with a PGA equal to  $0.35 \text{ m/s}^2$  while for a near-field scenario the PGA equals to  $0.8 \text{ m/s}^2$ . The soil type is chosen as rock-like, from documented reports of experimental testing on soil specimens [11]. Moreover, type 2 spectrum (near-field), is observed to be more significant, thus the structure's behaviour is more critical if analysed for this type of earthquake [12].

Incremental dynamic analysis is then performed for all three accelerograms and various scale factors, from the initial time-history response which corresponds to a scale factor of 1, until a scale factor of 3. The hysteretic curves of the first accelerogram are plotted for all scale factors, which are recorded as a horizontal displacement to normalized base shear relation (given by  $\alpha$ ). Main objective is the average IDA curve to be compared with the pushover curve of the chosen control node at the crown of the central span, which being located in the most distant position of all structural supports makes it more prone to larger displacements.

Firstly, the comparison between pushover and dynamic analysis shows that the stiffness of the pushover curve lies within the hysteretic curves following a similar slope (Fig.10).

Later on, an average IDA curve is plotted for two cases; one for the average value of all maximum displacements and their corresponding base shear coefficients, and one for maximum base shear coefficients and their corresponding displacements respectively, in order to investigate which of the two provides the best approximation to the horizontal capacity curve obtained by the pushover. The selection of maximum displacements for each relevant IDA curve is more appropriate for the multi-span bridge, since large displacements are more critical for their structural behaviour than maximum load factors.

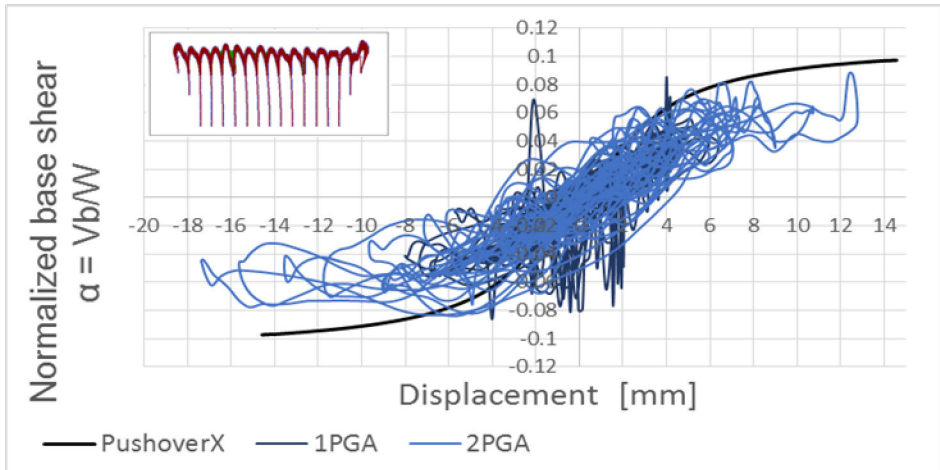


Fig. 10. Comparison between pushover and nonlinear dynamic analysis in the X-direction.

However, it is observed from Fig. 11 that for the first case, the points representing single dynamic simulations for different scale factors, are below the pushover curve showing lower stiffness, whereas for maximum load, the points are scattered around the pushover curve, resulting to an average IDA curve that presents a quite similar response to the capacity curve obtained by the pushover. Even though the results of the second case provide a good approximation indicating reliability in the model, more points for a larger variety of scale factors are necessary for this type of comparison, in order for the model to be trustworthy.

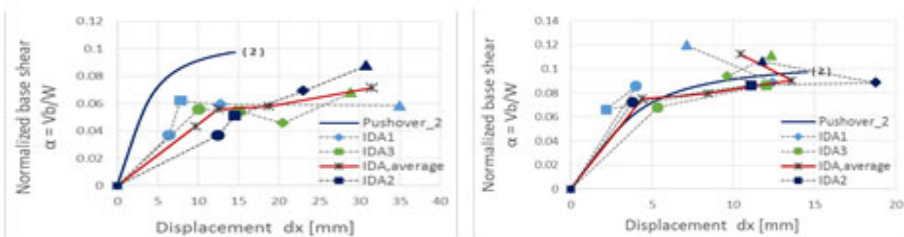


Fig. 11. IDA curves and capacity curves for earthquake in X-direction given for: left - maximum displacements; right - maximum base shear coefficients.

## 6. CONCLUSIONS

In this paper, through the fibre beam approach it is found that a proper discretization of the numerical model highly influences the maximum capacity of the structure. Application of this methodology to an experimental case leads to a good estimation of the maximum capacity but proves to be much stiffer than in reality, probably due to damage induced in the bridge prior to testing. In addition, the software is able to provide a curvature profile that demonstrates similar failure mechanisms in both experimental and numerical model. After validating the numerical model for simpler cases, it achieves a successful calibration of the first longitudinal mode when applied to the Durrães viaduct. From the pushover analysis it is observed that the choice of application point of horizontal incremental loads affects the total response. As a further step, from the IDA analysis, a good agreement is observed for the case of average IDA curve compared to the pushover, obtained for maximum load factor instead of displacement. Finally, while further development of the study is proven necessary, a good compromise between accuracy and simplicity has been achieved, thus the time needed for a time-history analysis is much reduced providing lower computational costs.

## ACKNOWLEDGEMENTS

Authors would like to acknowledge Dr. Stefano de Santis (Roma Tre University, Italy) for the useful discussions, and Prof. Matthew Gilbert (University of Sheffield, UK) whom has provided valuable experimental information regarding the Bolton Institute bridge test. Authors are also grateful to the SAHC Erasmus Mundus Masters programme for the Scholarship granted to the first author.

## REFERENCES

- [1] OPPENHEIM I. J., The Masonry Arch as a Four-Link Mechanism under Base Motion, *Earthquake Engineering and Structural Dynamics*, 1992, pp. 1005-1017.
- [2] MELBOURNE C., GILBERT M. and WAGSTAFF M., The Collapse Behaviour of Multispan Brickwork Arch Bridges, *Structural Engineer*, 1997, pp. 297-305.
- [3] DE SANTIS S., DE FELICE G., Seismic Analysis of Masonry Arches, *Proceedings of the fifteenth world conference on earthquake engineering*, 2012.
- [4] TAUCER F. F., SPACONE E. and FILIPPOU F. C., A Fiber Beam-Column Element for Seismic Response Analysis, *Engineering*, 1991, pp. 45-61.
- [5] SEPE V., SPACONE E., RAKA E. and CAMATA G., *Seismic Analysis of Masonry Buildings: Equivalent Frame Approach with Fiber Beam Element*, 2014, pp. 234-244.
- [6] TERZIC V., Force-based Element vs. Displacement-based Element, *OpenSees*, 2011, pp. 6-9.
- [7] MAZZONI S. and MCKENNA F., *OpenSees Command Language Manual*, *OpenSees*, 2006, pp. 57-61.
- [8] DE SANTIS S., *Load-carrying Capability and Seismic Assessment of Masonry Bridges*, Ph.D. Dissertation, Roma Tre University, Rome, Italy, 2011, pp. 83-246.

- [9] COSTA C., RIBEIRO D., JORGE P. and SILVA R., Avaliação Experimental e Numérica dos Parâmetros Modais da Ponte Ferroviária de Durrães, *5as Jornadas Portuguesas de Engenharia de Estruturas*, 2014, pp. 1-12.
- [10] EN n.d., Eurocode 8: Design of structures for earthquake resistance – Part 1: General rules, seismic actions and rules for Buildings, *European Standard*, 2004.
- [11] MOREIRA V., *Avaliação de Segurança de Pontes Existentes. Aplicação ao Viaduto Ferroviário de Durrães*, M.Sc. Dissertation, 2014, pp. 115-132.
- [12] KYRIAKOU M., *Seismic Assessment of Masonry Arch Bridges with Fiber Element Strategy*, M. Sc. Dissertation, Portugal, 2015, pp. 79-85.